

## Research Article

---

# Crystallization, Polymorphism and Stability of Nanostructured Lipid Carriers Developed with Soybean Oil, Fully Hydrogenated Soybean Oil and Free Phytosterols for Food Applications

Valeria da Silva Santos<sup>1\*</sup>, Eriksen Koji Miyasaki<sup>1</sup>, Lisandro Pavie Cardoso<sup>2</sup>, Ana Paula Badan Ribeiro<sup>3</sup>, Maria Helena Andrade Santana<sup>1</sup>

<sup>1</sup>Department of Biotechnological Processes, School of Chemical Engineering, University of Campinas, Campinas, SP, Brazil

<sup>2</sup>Department of Applied Physics, Institute of Physics Gleb Wataghin, University of Campinas, Campinas, SP, Brazil

<sup>3</sup>Department of Food Technology, School of Food Engineering, University of Campinas, Campinas, SP, Brazil

**\*Corresponding Author:** Valeria da Silva Santos, Department of Biotechnological Processes, School of Chemical Engineering, University of Campinas, 500 Albert Einstein Ave., Campinas, SP 13083-970, Brazil, Tel: +55 019 984072784; E-mail: [santosilvaleria@hotmail.com](mailto:santosilvaleria@hotmail.com)

**Received:** 30 May 2019; **Accepted:** 11 June 2019; **Published:** 14 June 2019

## Abstract

The aim of this work was the development of nanostructured lipid carriers (NLC) using conventional fats and oils (soybean oil, SO and fully hydrogenated soybean oil, FHSO) for incorporation of free phytosterols (FP). FP are lipophilic bioactive compounds which can reduce blood cholesterol levels, through a competitive mechanism of absorption, aiding in the prevention of cardiovascular diseases. However, FP presents difficulties related to technological applications in foods due to the high melting point. In this way, NLC can be a means of making feasible incorporation of FP in foods. NLC were obtained in aqueous dispersion through the emulsification process, followed by high-pressure homogenization (HPH) using 3 and 5 cycles at 800 bar, with subsequent crystallization and stabilization of the lipid matrices (LM). The emulsifiers used were soybean lecithin (SL), ethoxylated sorbitan monooleate (T80) and sorbitan monostearate (S60). The thermal and crystalline behavior of the LM, FP and NLC were evaluated. NLCs were characterized by size and polydispersity. FP presented high crystallization (126°C) and melting (137°C) temperatures, but this did not avoid its incorporation into NLC. The NLC presented size between 154 to 534 nm and polydispersity ranging from 0.1 to 0.5, the lower limits being obtained with the T80. NLC were found to require lower temperatures to crystallize and polymorphic transitions were accelerated. This study indicated that the conventional raw materials were compatible with the development of NLC with FP.

**Keywords:** Nanotechnology; Foods; Nanostructured Lipid Carriers; Free phytosterols; High-pressure homogenization

## **1. Introduction**

Lipids have been used as raw material for nanoparticles development, mainly for the solubilization capacity of lipophilic bioactive compounds. In addition, lipid nanoparticles may improve the chemical stability and permeability of bioactive compounds through the gastrointestinal tract (GIT) and may also facilitate its absorption [1-3]. There are currently two types of lipid nanoparticles, solid lipid nanoparticles (SLN) developed with saturated lipids and nanostructured lipid carriers (NLC) composed of both saturated and unsaturated lipids. NLC were developed to overcome possible limitations associated with the SLN. The insertion of unsaturated lipids was performed to produce less structured lipid matrices, in relation to crystallinity, obtaining a better incorporation efficiency and avoiding the release/expulsion of bioactive compounds during storage [4-5]. The lipid matrices of the NLC are generally produced with high-cost lipids, such as purified triacylglycerols (TAGs) and/or synthetic lipid materials [6]. These matrices make NLC economically unfeasible when considering the scale and possibility of application in food systems. Thus, the combination of the characteristics from the lipid sources commonly applied in the food industry, such as vegetable oils and fats, seems to be promising for the development of nanostructured lipid systems.

High potential and low-cost option for application in this kind of systems are the fully hydrogenated vegetable oils, also known as hardfats. These materials are obtained when all the double bonds of the fatty acids are saturated during the total catalytic hydrogenation process of unsaturated oils. Hardfats have been developed as a raw material to replace partially hydrogenated fat, contributing to the development of interesterified low-trans fats by means of the interesterification process. Currently, hardfats have been also the object of studies focused on the modification of fat physical properties, as well as the structuring of liquid oils [7, 8]. In this way, the use of hardfats combined with polyunsaturated oils such as soybean, canola, and sunflower oil is a promising option for the development of LM for the incorporation of lipophilic bioactive compounds, such as free phytosterols (FP) in NLC. The FP is considered a functional compound because it establishes a competitive mechanism during the absorption of cholesterol, reducing cholesterol blood levels, which is closely related to the prevention of cardiovascular diseases and reduction of cancer risk [9, 10]. However, FP has high crystallinity and low solubility in water, so few FP products are available for consumption, mainly due to technological application issues [11].

It is important to consider that when the raw materials involved in the processing of nanoparticles are oils and fats, the main points of studies are related to the crystallization behavior and lipid polymorphism. These properties are influenced by intrinsic and extrinsic factors, such as chemical composition, production process, thermal recrystallization conditions, among others. Conventional lipids, unlike purified materials, are composed of a variety of TAGs groups with different requirements for nucleation energy, molecular diffusion, and the crystal network establishment for each application [12]. The crystallization behavior and the polymorphic transitions of lipid materials at the nanoscale, for the development of NLC, is still unclear, but it is directly related to the physical

stability [13]. The main objective of this work was to develop NLC with conventional raw materials, such as SO and FHSO for the incorporation of FP. In addition, the crystallization and polymorphism of the LM and NLC were evaluated to verify the influence of these properties on the physical stability of NLC. This NLC development approach, with vegetable oil and hardfats for incorporation of bioactive compounds, is totally unprecedented. Giving the authors of this work a patent under the privilege of the invention under registration in the National Institute of Industrial Property-INPI (BR 10 2017 006471 9) [13].

## **2. Materials and Methods**

### **2.1 Materials**

Refined SO was locally purchased, FHSO was supplied by SGS (Brazil) and the FP was courtesy of a local production initiative. The emulsifiers used were deoiled SL composed of 68-73% phosphatidylcholine and a hydrophilic-lipophilic balance (HLB) of 7.0 obtained from Solae Company (St. Louis, MO, USA), S60 of HLB 4.7, from Sigma-Aldrich® and T80 of HLB 15.0, donated by Croda (Brazil).

### **2.2 Methods**

**2.2.1 Fatty acid composition:** The fatty acid composition (FAC) of the raw materials was carried out in triplicate by gas chromatography with capillary column according to the method AOCS Ce 1f-96 [14]. After esterification using Hartman and Lago [15] the fatty acid methyl esters were separated on Agilent DB-23 column (50% cyanopropyl-methyl polysiloxane), with dimensions of 60 m, internal diameter: 0.25 mm, 0.25 µm film. Chromatographic conditions: oven temperature 110°C/5 min, 110°C-215°C (5°C/min), 215°C-24 min; detector temperature: 280°C; injector temperature: 250°C; carrier gas: helium; split ratio: 1:50; volume injected: 1.0 µL. The qualitative composition was determined by comparing the retention times of the peaks with those of the respective fatty acid standards, while the quantitative composition was performed by area normalization, according to the recommendation of the cited method.

**2.2.2 Triacylglycerol composition:** The determination of TAGs composition of the raw materials was performed in triplicate by dissolving the sample in tetrahydrofuran (THF, 20 mg/mL) and injecting into a gas chromatograph equipped with capillary column Agilent Catalog 122-1811 DB-17HT (50%-phenylmethyl polysiloxane), with 15 meters, 0.25 mm of internal diameter and 0.15 µm of film. Analysis conditions: split injection, ratio 1:100; column temperature: 250°C, programmed to 350°C at 5°C/min; carrier gas: helium, at a flow rate of 1.0 mL/min; injector temperature: 360°C; detector temperature: 375°C; volume injected: 1.0 µL. The identification of the TAGs groups was performed by comparing the retention times, according to the procedures of Antoniosi et al. [16], and the quantification of the groups was performed by area normalization as recommended by the authors.

**2.2.3 Free phytosterols profile:** To obtain the FP profile, the unsaponifiable matter was first extracted by the Ca 6a-40 method, and then, using the Ch 6-91 method, the sterol profile was determined, and the total sterol content was quantified by means of using internal standard  $\alpha$ -cholestanol (1 mg/kg Sigma-Aldrich) [14], procedures performed

in triplicate. Data were expressed as the total percentage of phytosterols in the sample, using the ratio of the internal standard peak area, and the total phytosterols peak area, according to the recommendation of the method. Peak identification was performed by calculation of the retention time and comparison with the standard chromatogram. The FP profile was obtained by the ratio of each phytosterol peak area and the total phytosterols peak area.

**2.2.4 Formulations:** NLC were prepared with 10% (m/m) of the lipid phase and 90% (m/m) of the aqueous phase. The aqueous phase was composed of distilled water and 2% of emulsifier according to Santos et al. [13]. Regarding the lipid phase, NLC was developed with lipid matrices composed of 50% of liquid lipid (SO) and 50% of solid lipid (FHSO). For NLC with the incorporation of the bioactive compound, the liquid lipid was partially replaced by 30% of FP. The emulsifiers SL, S60 and T80 were used separately in each formulation for evaluation of their individual behavior (Table 1).

ID <sup>a</sup>	Lipid Fraction (10% of the general formulation) <sup>b</sup>		Emulsifier	HPH cycles
	Lipid matrix (%)	Bioactive Compound (%)		
NLC <sub>T80</sub>	50 SO + 50 FHSO	-	T80	3
NLC <sub>S60</sub>	50 SO + 50 FHSO	-	S60	3
NLC <sub>SL</sub>	50 SO + 50 FHSO	-	SL	3
NLC <sub>T80</sub>	50 SO + 50 FHSO	-	T80	5
NLC <sub>S60</sub>	50 SO + 50 FHSO	-	S60	5
NLC <sub>SL</sub>	50 SO + 50 FHSO	-	SL	5
NLC +FP <sub>T80</sub>	20 SO + 50 FHSO	30 FP	T80	3
NLC +FP <sub>S60</sub>	20 SO + 50 FHSO	30 FP	S60	3
NLC +FP <sub>SL</sub>	20 SO + 50 FHSO	30 FP	SL	3
NLC +FP <sub>T80</sub>	20 SO + 50 FHSO	30 FP	T80	5
NLC +FP <sub>S60</sub>	20 SO + 50 FHSO	30 FP	S60	5
NLC +FP <sub>SL</sub>	20 SO + 50 FHSO	30 FP	SL	5

<sup>a</sup>NLC: Nanostructured Lipid Carriers; NLC+FP: Nanostructured Lipid Carriers with Free Phytosterols; T80: Formulation containing 2% of emulsifier ethoxylated sorbitan monooleate; S60-Formulation containing 2% of emulsifier sorbitan monostearate; SL-Formulation containing 2% of emulsifier soybean lecithin; HPH-high-pressure homogenization; <sup>b</sup>NLC were prepared with 10% (m/m) of lipid phase and 90% (m/m) of the aqueous phase composed of water and 2% emulsifier.

**Table 1:** Lipid nanoparticle formulations, including lipid matrices, bioactive compound and emulsifiers and the number of high-pressure homogenization at 800bar.

**2.2.5 Production process:** The preparation of the lipid matrices consisted of the mixture of the liquid lipids (SO), solids lipids (FHSO), and FP, according to each formulation described in Table 1. Each mixture was stirred, on a magnetic stirrer at 300 rpm/2 min at 90°C. Thereafter, they were conditioned under specific conditions for further

characterization. To obtain the NLC and NLC+FP, the lipid matrices were prepared with the subsequent addition of the aqueous phase containing the emulsifier, at the same temperature (90°C). The pre-emulsion was obtained in Ultra Turrax IKA T18 Basic (Germany) at 20,000 rpm/3 min. Then, pre-emulsions were subjected to hot homogenization in a high-pressure homogenizer (HPH) (GEA Niro Soavi, model: NS 1001L PANDA 2K, Italy) at 800bar and 90°C under two different conditions: 3 and 5 cycles (Table 1), according to Santos et al. [13]. After the HPH process, the obtained nanoemulsions were cooled to 5°C/24 h for crystallization of the lipid fraction followed by crystal stabilization at 25°C/24 h, obtaining the dispersions of NLC and NLC+FP, according to formulations described in Table 1.

**2.2.6 Drying processes of NLC:** The nanoparticles obtained after HPH were submitted to two different drying processes: (a) Heating-the nanoparticles in aqueous dispersion were exposed for 24 h in a drying oven with air circulation at 40°C (Q317M, Brazil); (b) Lyophilization-the aqueous dispersion containing the nanoparticles was first conditioning in ultrafreezer at -80°C/24 h in order to freezing the aqueous phase, followed by lyophilization (Liobras L101, Brazil), according to the method described by Zimmermann et al. [17].

**2.2.7 Thermal analysis:** The thermal analyzes were performed in the nanoparticles in aqueous dispersion and in the LM using Transmission Differential Calorimetry (DSC) TA Instruments, model Q2000, coupled to the RCS90 refrigeration system (TA Instruments, Waters LLC, New Castle). The data processing system used was Universal V4.7A (TA Instruments, Waters LLC, New Castle), and the analysis conditions are described in the sequence.

**2.2.8 Lipid matrices:** The official method of AOCS Cj 1-94 [15] was used, with a maximum the temperature changed from 80°C to 150°C due to the high melting point of FP. The conditions of analysis were: sample mass: ~10 mg; Crystallization events: 150°C/10 min, 150°C to -40°C (10°C/min); Melting events: -40°C/30 min, -40°C to 150°C (5°C/min). The following parameters were used to evaluate the results: initial crystallization and melting temperatures ( $T_{ic}$  and  $T_{im}$ ), peak crystallization and melting temperatures ( $T_{pc}$  and  $T_{pm}$ ), enthalpies of crystallization and melting ( $\Delta H_c$  and  $\Delta H_m$ ) and final temperature of crystallization and melting ( $T_{fc}$  and  $T_{fm}$ ) [18].

**2.2.9 Nanoparticles in aqueous suspension:** Cooling-heating-cooling cycles (37-5-75-5°C) adapted from Awad et al. [1], were used to study the crystallization behavior and stability. Approximately 10 mg of samples were packed in hermetic aluminum pans at 37°C shortly after HPH and were immediately analyzed under inert atmosphere ( $N_2$ ) under the following conditions: start temperature 37°C cooling to 5°C followed by heating to 75°C and soon after being cooled again at 5°C, using a constant rate of 10°C/min during all cycles. The following parameters were used to evaluate the results: initial crystallization and melting temperature ( $T_{ic}$  and  $T_{im}$ ), peak crystallization and melting temperatures ( $T_{pc}$  and  $T_{pm}$ ), recrystallization temperature ( $T_{rc}$ ), enthalpies of crystallization and melting ( $\Delta H_c$  and  $\Delta H_m$ ), enthalpy of recrystallization ( $\Delta H_{rc}$ ) and completion temperature of crystallization, melting and recrystallization ( $T_{fc}$ ,  $T_{fm}$ ,  $T_{frc}$ ) [18].

**2.2.10 Particle size and Polydispersity Index:** The particle size of the nanoparticles was obtained by means of the hydrodynamic diameter (Z-ave) in nanometers (d.nm) using dynamic light scattering (DLS) with a high-power laser in Zetasizer Nano NS equipment, Malvern, United Kingdom. The nanoparticles were evaluated in triplicate for the Z-ave and PDI after 24 h and 15 days of the production process. The samples were diluted with distilled water to reduce the opalescence before the determinations. Data analyzes were performed using the software included in the equipment system.

**2.2.11 X-ray diffraction:** The X-ray diffraction (XRD) of LM and the dried nanoparticles were determined according to the AOCS method Cj 2-95 [14]. Previously, the LM was melted at 130°C, crystallized at 5°C/24 h followed by stabilization at 25°C/24 h. The measurements were carried out in a Philips diffractometer (PW1710) using Bragg-Brentano ( $\theta:2\theta$ ) geometry with Cu- $\alpha$  radiation ( $\lambda=1.54056 \text{ \AA}$ , 40 KV voltage and 30 mA current). The measurements were obtained at 25°C with steps of 0.02° in 2° and an acquisition time of 2 seconds, with scans of 1.8 to 40° (2° scale). The identification of the polymorphic forms of triacylglycerols was performed from the Short Spacing (SS) characteristic of the lipid crystals [14].

**2.2.12 Statistical analysis:** Data were statistically analyzed by means of One-Way Analysis of Variance (ANOVA) with the Statistica (V.7) Software (Statsoft Inc., Tulsa, UK). The Tukey test was applied to determine the significant differences between the means, at a level of  $p \leq 0.05$ .

### 3. Results and Discussion

#### 3.1 Chemical characterization

In the FAC of the SO, the predominant content of unsaturated fatty acids was 53.32% of linoleic acid (C18:2), 23.38% of oleic acid (C18:1) and 6.66% and linolenic acid (C18:3). Regarding the saturated fatty acids, 10.70% of palmitic acid (C16:0) and 4.26% of stearic acid (C18:0), were predominated (Table 2). Similar values were reported by Ribeiro et al. [19], but it is also possible to find SO with very broad ranges of unsaturated fatty acids, such as 48-59% linoleic acid, 17-30% oleic acid and 4.5-11% linolenic acid [20].

Fatty acids (%)	SO <sup>a</sup>	FHSO <sup>a</sup>
C16:0 - Palmitic acid	10.70 ± 1.12	11.22 ± 0.50
C16:1 - Palmitoleic Acid	0.09 ± 0.02	-
C18:0 - Stearic Acid	4.26 ± 0.26	87.11 ± 0.06
C18:1 - Oleic Acid	23.38 ± 0.96	-
C18:2 - Linoleic Acid	53.32 ± 0.58	-
C18:3 - Linolenic Acid	6.66 ± 0.10	-
C20:0 - Arachidonic acid	0.41 ± 0.03	0.60 ± 0.18
C22:0 - Behenic acid	-	0.75 ± 0.28
Σ Saturated	15.83	100

Σ unsaturated	83.45	<1
---------------	-------	----

<sup>a</sup>Average of three replicates ± Standard Deviation. Values below 0.2% were omitted from the table.

**Table 2:** Fatty acid composition of soybean oil (SO) and fully hydrogenated soybean oil (FHSO).

During the process of total hydrogenation of oils, the unsaturated fatty acids are transformed into saturated fatty acids [7]. Thus, the high content of stearic acid (C18:0) found as a major in FHSO is a consequence of the complete hydrogenation process of SO, which naturally contains high concentrations of unsaturated fatty acids with 18 carbons [21]. The FHSO presented 87.11% of stearic acid (C18:0), 11.22% of palmitic acid (C16:0), with small proportions of arachidonic and behenic acids (Table 2). Metabolically, stearic acid is basically used as an energy source, with no influenced the metabolism of hormones, prostaglandins, and leukotrienes.

In addition, it has no adverse effect on the risks of cardiovascular diseases, it has no atherogenic effect [21]. The SO had 14 TAGs species, while in the FHSO only 5 were found. The predominant TAGs in the SO were PLO, PLL, OLL, LLL, and LLnL, corresponding to 80.26% of the total content, whereas in FHSO only PSS (28.84%) and SSS (66.21%) were found, as expected (Table 3). In the literature, similar values are observed for the same TAGs in FHSO, varying between 90 and 95% of the total TAG content [22].

NC	TAG	SO (%)	FHSO (%)
50	PPS	-	3.19 ± 0.35
	POP	1.58 ± 0.35	-
	PLP	4.63 ± 0.39	-
52	PSS	-	28.84 ± 0.92
	POS	1.03 ± 0.10	-
	POO	6.52 ± 0.54	-
	PLO	13.25 ± 1.13	-
	PLL	19.28 ± 1.86	-
	PLnL	2.39 ± 0.69	-
54	SSS	-	66.21 ± 1.46
	SOO	1.30 ± 0.77	-
	SLO	2.25 ± 0.28	-
	OLO	2.51 ± 0.50	-
	OLL	11.55 ± 0.91	-
	LLL	17.35 ± 1.10	-
	LLnL	18.83 ± 1.21	-
	LLnLn	2.59 ± 0.38	-
56	EEA	-	0.49 ± 0.28
58	SSBe	-	1.28 ± 0.09

Total		100	100
-------	--	-----	-----

NC-Number of carbons; P-palmitic acid; S-stearic acid; O-oleic acid; L-acid linoleic; Ln-linolenic acid; A-acid arachidonic; Be-behenic acid; --not detected

**Table 3:** Triacylglycerols composition of soybean oil (SO) and fully hydrogenated soybean oil (FHSO).

The FP composition was determined only in the lipophilic bioactive compound since in the other lipid components this content is irrelevant, less than 1% [23]. The FP is 98% pure and the components with the highest concentrations were  $\beta$ -sitosterol, stigmasterol, and campesterol, with contents of 44.05, 26.77 and 23.53%, respectively, as can be seen in Table 4.

Composition of free phytosterols	(%) <sup>a</sup>
Cholesterol	0.60 ± 0.02
Brassicasterol	0.30 ± 0.01
Campesterol	23.56 ± 0.23
Campestanol	0.66 ± 0.11
Stigmasterol	26.77 ± 0.22
$\Delta$ -7-Campesterol	0.78 ± 0.04
$\Delta$ -5,23- Stigmastadienol	0.48 ± 0.01
$\beta$ -Sitosterol	44.05 ± 0.15
Sitostanol	1.18 ± 0.08
$\Delta$ -5-Avenasterol	0.84 ± 0.04
$\Delta$ -5-24-Stigmastadienol	0.14 ± 0.01
$\Delta$ -Stigmastenol	0.47 ± 0.02
$\Delta$ -7-Avenasterol	0.68 ± 0.01
Total of phytosterols	98.00

<sup>a</sup>Average of three replicates ± Standard Deviation

**Table 4:** Sterols profile of the bioactive compounds loaded in the lipid nanoparticles.

### 3.2 Thermal characterization

**3.2.1 Crystallization behavior of lipid matrices:** The SO was liquid at room temperature and during NLC production, because it is composed mainly of the unsaturated fatty acids (linoleic and oleic) which present low melting points [22]. Therefore, the SO is a suitable raw material for use as liquid lipid in NLC and of great potential for application in these systems, replacing synthetic liquid LM, mainly in terms of cost in the food industry scenario. In the crystallization of FHSO, only one peak was observed, reaching maximum crystallization at 47°C. This behavior was also reported by [7], it is directly related to the chemical composition, since FHSO is composed of approximately 87% of stearic acid. Mensink [24] and Tamjidi et al. [25] have reported that lipid mixtures rich in stearic acid represent raw materials of great importance for lipid nanoparticles composition since it presents a

melting point higher than body temperature and also because stearic acid is considered metabolic neutral. The mixture of SO and FHSO in the proportion of 50% of each, showed a single peak at 43.09°C. Some authors have reported that the combined use of solid and liquid lipid fractions in lipid nanoparticles is important to maintain structural and stability characteristics. In addition, for incorporation of bioactive compounds, the use of both, liquid and solid lipids, is positive, since it allows the elaboration of LM with a low crystallinity degree, offering more spaces to accommodate the bioactive compound in nanoparticles structures, as well as to minimize the undesired expulsion of the bioactive compound during possible polymorphic transitions [25, 26].

**3.2.2 Crystallization behavior of FP:** A peak crystallization was observed, with  $T_{pc}$  of approximately 126°C and a melting peak at 137.94°C, indicating that the predominant fraction of the FP components have similar crystallization and melting properties (Table 5). However, between 50 and 60°C, some exothermic and endothermic transitions were observed, but at low intensities (Figure 1).

Samples	$T_{ic}$ (°C)	$T_{pc}$ (°C)		$\Delta H_c$ (J/g)		$T_{fc}$ (°C)
		Peak 1	Peak 2	Peak 1	Peak 2	
FHSO	50.41	47.75	nd <sup>a</sup>	123.00	nd	25.91
FP	126.41	126.37	nd	41.96	nd	119.72
SO+FHSO	44.83	43.09	nd	72.76	nd	19.70
SO+FHSO <sub>T80</sub>	45.47	43.03	nd	67.16	nd	19.89
SO+FHSO <sub>S60</sub>	43.48	41.68	nd	61.46	nd	17.29
SO+FHSO <sub>SL</sub>	43.69	42.09	nd	41.75	nd	18.36
SO+FHSO+FP	47.13	45.34	nd	94.93	nd	20.94
SO+FHSO+FP <sub>T80</sub>	65.06	59.06	43.48	44.42	52.12	49.13
SO+FHSO+FP <sub>S60</sub>	40.17	38.57	nd	56.28	nd	21.05
SO+FHSO+FP <sub>SL</sub>	81.25	75.13	45.06	31.29	44.27	70.52

<sup>a</sup>nd-not detected

**Table 5:** Crystallization behavior of the lipid raw material and their blends with emulsifiers and FP, used in the production of NLC. Initial crystallization temperature ( $T_{ic}$ ), peak crystallization temperature ( $T_{pc}$ ), enthalpy of crystallization ( $\Delta H_c$ ) and final crystallization temperature ( $T_{fc}$ ).

Vaikousi et al. [9] observed similar events with peaks close to 60°C and also 97 and 105°C. According to these authors, these thermal events may be related to the loss of hydration water from the crystals remained from the FP obtaining process, that undergoes repeated washes with aqueous solutions.

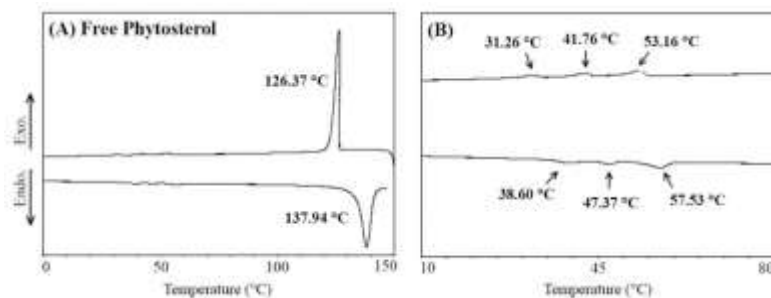


**Figure 1:** Crystallization and melting curves of the free phytosterols (A) and zoom of the region with peaks of lower intensities; (B) obtained by differential scanning calorimetry (DSC).

Firstly, a part of the hydration water is lost, and semi-hydrated crystals are formed (below 60°C), while the remainder of the hydration water leaves the crystal at approximately 90°C. As seen, FP has a high melting point, and, in addition, the present water insolubility, characteristics that result in the great technological challenge for food applications. As reported by Hariklia Vaikousi et al. [9] in their studies, the direct delivery of FP in food is considered a technological challenge, since the high crystallinity/insolubility can often become a restrictive factor for the physical stability of several products. Thus, the incorporation of FP into NLC can be a viable alternative for the enrichment of several food products. In NLC the FP are solubilized in the LM and assume a different physical behavior, as can be observed in Figure 2 and Table 5, discussed below.

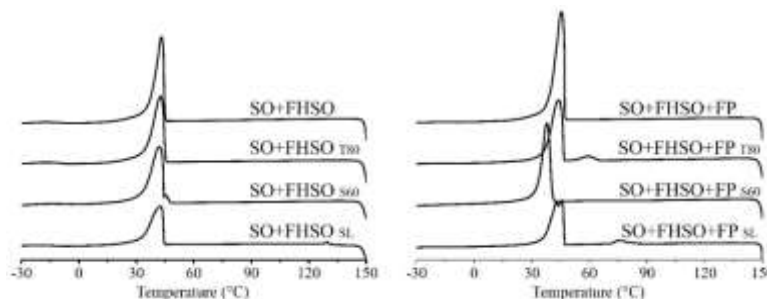


**Figure 2:** Crystallization behavior obtained from differential scanning calorimetry (DSC) of the lipid matrices composed by soybean oil (SO) and fully hydrogenated soybean oil (FHSO) and their mixtures containing the three different emulsifiers (soybean lecithin-SL, polyethoxylated sorbitan monooleate-T80 and sorbitan monostearate-S60) and free phytosterols (FP), by cooling from 150 to -40°C for samples with FP and by 80 to -40°C for others lipid matrices.

**3.2.3 LM crystallization behavior in the presence of FP:** Only one crystallization peak was observed, with  $T_{oc}$  of 45.34°C. Thus, it is affirmed that FP was incorporated by the LM, as set forth in Table 5. Furthermore, evaluating the impact of the FP in the LM crystallization, it is possible to observe that the crystallization peak present in the thermogram varies in position, shape, and magnitude. Analyzing the parameters in Table 5, the addition of FP promoted the acceleration of the crystallization and increase the  $\Delta H_c$  from 72.76 to 94.93 J/g, contributing to the increase of the thermal resistance of the LM.

**3.2.4 Influence of emulsifiers on the crystallization behavior of LM:** Small influences of the emulsifiers were observed at the  $T_{oc}$  of the mixtures containing SO and FHSO (44.83°C), the presence of T80 delayed the initial crystallization to 45.47°C, while S60 and SL have anticipated the crystallization event to 43.48 and 43.69°C respectively (Table 5). In the LM containing T80 and SL, two crystallization peaks were observed, with different intensities, the second being more intense than the first (Figure 2). This effect may be related to the possible induction of FP crystallization caused by the presence of emulsifiers. The acceleration of crystallization was observed through the  $T_{pc}$  for peak 1 of each sample, from 45.34°C to 59.06 and 75.13°C, for T80 and SL respectively. However, the higher phase transitions were observed in the second peaks, which presented higher values for the  $\Delta H_c$  (Table 5). A different behavior was verified in the presence of S60, in which the crystallization curve showed only one peak (Figure 2); the values obtained for  $T_{oc}$  and  $T_{pc}$  indicate that this emulsifier has delayed the crystallization of the lipid matrix in the presence of FP and the  $\Delta H_c$  was not affected (Table 5). Differentiated behaviors were observed during the crystallization of the LM in the presence of emulsifiers. The results agree with the literature, which indicates that the presence of certain emulsifiers interferes with the crystallization behavior of lipid materials, slowing or speeding up this process [27].

**3.2.5 Production process:** The HPH method used to produce NLC and NLC+FP proved to be efficient for the developed systems. It was possible to obtain NLC with desirable colloidal characteristics using 3 and 5 cycles of homogenization at 800bar, according to results presented and discussed in the following topic. It is important to highlight that, the emulsifiers used in the nanoparticle formulations combined with the production method, have a great influence on the obtention, viability, and stabilization of the aqueous dispersions. It was observed that the SL emulsifier was not compatible with the FP containing formulation since during the pre-emulsion stage the system showed high viscosity limiting processing in HPH. The other systems remained liquid, no viscosity increase during processing.

**3.2.6 Particle size and Polydispersity Index:** In Figure 3 and 4, it is possible to observe the particle size distribution expressed according to intensity ( $I\alpha d^6$ ) and number ( $N\alpha d$ ), for the systems developed with 3 and 5 cycles of HPH. The results were expressed in terms of scattered light intensity, I distribution, the proportional diameter to the sixth power ( $I\alpha d^6$ ), and in terms of the number of particles, N distribution, proportional to the predominant diameter in the sample ( $N\alpha d$ ).

The  $NLC_{T80}$  and  $NLC+FP_{T80}$  obtained at 3 and 5 cycles, analyzed after 24 h of production, had a Z-ave of approximately 164 nm, with no significant difference ( $p \geq 0.05$ ) between them. It was noted that the increase in the number of cycles (from 3 to 5 cycles) of homogenization did not interfere in the Z-ave. However, it was effective in reducing the PDI without the inclusion of the bioactive compound (Table 6). Similar behavior was observed for the  $NLC_{SL}$  evaluated after 24 h of the process, in which no significant differences were observed for both parameters in 3 and 5 cycles.

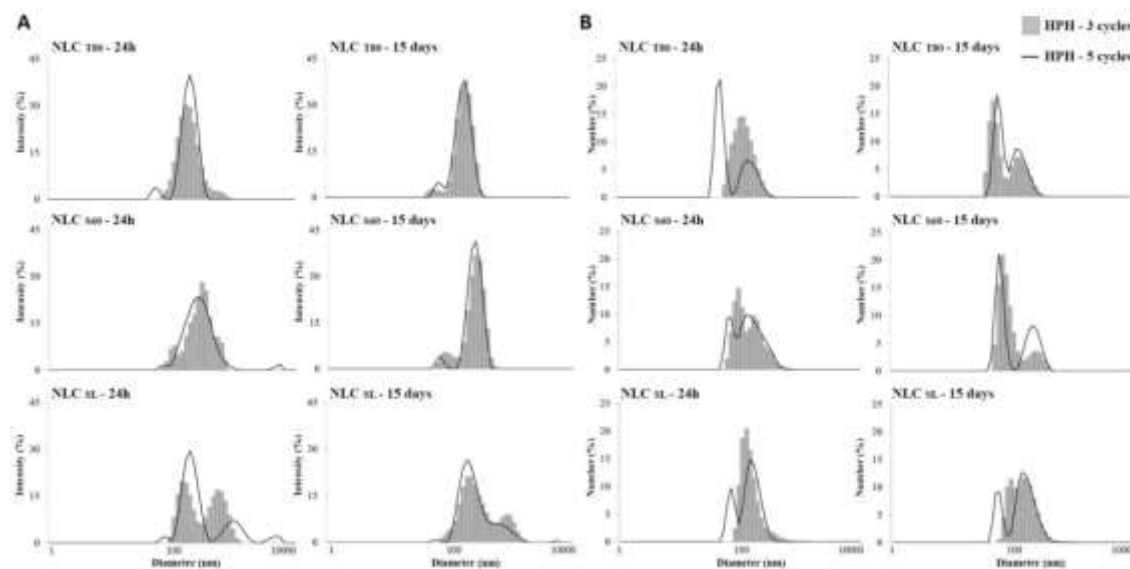


**Figure 3:** Hydrodynamic particle size distribution, Z-ave (d.nm) of the NLC with different emulsifiers: soybean lecithin-SL, polyethoxylated sorbitan monooleate-T80 and sorbitan monostearate-S60, submitted to 3 and 5 cycles of high-pressure homogenization (HPH), analyzed after 24 h and 15 days of production, expressed as (A) intensity ( $I_{ad}^6$ ) and (B) number ( $N_{ad}$ ).

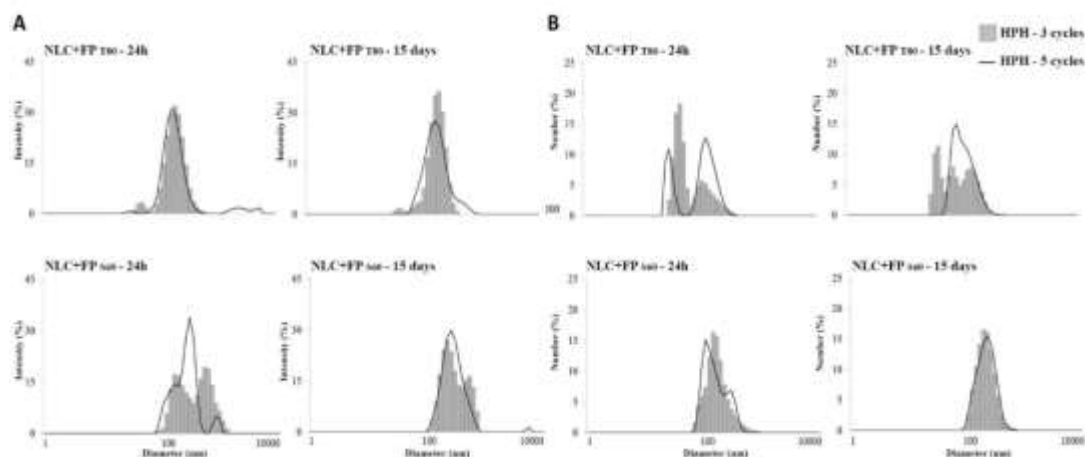


**Figure 4:** Hydrodynamic particle size distribution (d.nm) of the NLC+FP developed with different emulsifiers: soybean lecithin-SL, polyethoxylated sorbitan monooleate-T80 and sorbitan monostearate-S60, submitted to 3 and 5 cycles of high-pressure homogenization (HPH), analyzed after 24 h and 15 days of production, expressed as (A) intensity ( $I_{ad}^6$ ) and (B) number ( $N_{ad}$ ).

Samples <sup>1</sup>	Z-ave (d.nm) <sup>2</sup>	PDI <sup>2</sup>
<b>3 Cycles de HPH-24 h</b>		
NLC <sub>T80</sub>	167.34 ± 0.13 <sup>l</sup>	0.176 ± 0.009 <sup>dc</sup>
NLC <sub>S60</sub>	283.30 ± 5.31 <sup>cd</sup>	0.424 ± 0.056 <sup>abcd</sup>
NLC <sub>LS</sub>	250.20 ± 3.21 <sup>efg</sup>	0.346 ± 0.006 <sup>abcde</sup>

NLC+FP <sub>T80</sub>	164.97 ± 1.98 <sup>l</sup>	0.235 ± 0.006 <sup>cde</sup>
NLC+FP <sub>S60</sub>	437.60 ± 22.54 <sup>b</sup>	0.485 ± 0.086 <sup>ab</sup>
NLC+FP <sub>SL</sub>	-	-
<b>3 Cycles de HPH-15 days</b>		
NLC <sub>T80</sub>	161.15 ± 0.44 <sup>l</sup>	0.170 ± 0.002 <sup>e</sup>
NLC <sub>S60</sub>	215.47 ± 7.41 <sup>hi</sup>	0.212 ± 0.012 <sup>de</sup>
NLC <sub>LS</sub>	271.80 ± 2.32 <sup>cde</sup>	0.373 ± 0.005 <sup>abcde</sup>
NLC+FP <sub>T80</sub>	160.98 ± 1.95 <sup>l</sup>	0.254 ± 0.019 <sup>bcde</sup>
NLC+FP <sub>S60</sub>	297.60 ± 7.84 <sup>c</sup>	0.481 ± 0.071 <sup>abc</sup>
NLC+FP <sub>SL</sub>	-	-
<b>5 Cycles de HPH-24 h</b>		
NLC <sub>T80</sub>	160.79 ± 0.74 <sup>l</sup>	0.165 ± 0.007 <sup>e</sup>
NLC <sub>S60</sub>	259.80 ± 1.63 <sup>def</sup>	0.304 ± 0.020 <sup>bcde</sup>
NLC <sub>SL</sub>	228.47 ± 0.38 <sup>ghi</sup>	0.330 ± 0.005 <sup>bcde</sup>
NLC+FP <sub>T80</sub>	163.69 ± 2.80 <sup>l</sup>	0.269 ± 0.021 <sup>bcde</sup>
NLC+FP <sub>S60</sub>	681.70 ± 15.11 <sup>a</sup>	0.590 ± 0.244 <sup>a</sup>
NLC+FP <sub>SL</sub>	-	-
<b>5 Cycles de HPH-15 days</b>		
NLC <sub>T80</sub>	155.38 ± 1.00 <sup>l</sup>	0.144 ± 0.011 <sup>e</sup>
NLC <sub>S60</sub>	211.00 ± 1.88 <sup>l</sup>	0.170 ± 0.004 <sup>e</sup>
NLC <sub>SL</sub>	241.00 ± 2.24 <sup>lgh</sup>	0.342 ± 0.110 <sup>bcde</sup>
NLC+FP <sub>T80</sub>	154.82 ± 1.20 <sup>l</sup>	0.246 ± 0.012 <sup>bcde</sup>
NLC+FP <sub>S60</sub>	288.30 ± 5.14 <sup>c</sup>	0.307 ± 0.090 <sup>bcde</sup>
NLC+FP <sub>LS</sub>	-	-

<sup>l</sup>NLC: nanostructured lipid carriers; T80: Formulation containing 2% of emulsifier ethoxylated sorbitan monooleate; S60-Formulation containing 2% of emulsifier sorbitan monostearate; SL-Formulation containing 2% of emulsifier soybean lecithin; <sup>2</sup>Values represent the average of three replicates ± standard deviation. Different letters in the same column indicate significant differences by the Tukey test at the 5% probability level ( $p \leq 0.05$ ).

**Table 6:** Particle size in hydrodynamic diameter, Z-ave (d.nm) and polydispersity index (PDI) of NLC and NLC+FP evaluated after 24 hours and 15 days of production using 3 and 5 cycles of high pressure homogenization (HPH).

The use of S60 in NLC+FP produced from 3 and 5 cycles of HPH caused a significant increase ( $p \geq 0.05$ ) of Z-ave, (from 392 to 534 nm), as well as the PDI that assumed values above 0.4 (Table 6). So, the use of a greater number of HPH cycles for FP containing system was not suitable. According to Tamjidi et al. [25], the PDI is related to the physical stability of LN; PDI values should be in the range of 0.1 to 0.25 to provide dispersions with long-term stability, and values above 0.5 indicate very broad particle size distribution, characterizing low physical stability. Engel et al. [28] evaluated three different systems with tristearin, triolein and decanoic acid containing 2.0% of SL

as crystallization inhibitor and 2.5% of FP, dispersed in the aqueous phase containing 1.0% of polysorbate 20 in HAP at 1000 bar. The Z-ave obtained for each system was 131 nm, 100 nm, and 102 nm, respectively. The authors reported that FP had little influence on Z-ave while they are dispersed in the oil phase, however, when they come in contact with the aqueous phase, the crystallization of FP occurs and the Z-ave of the particles increases significantly, destabilizing the system (Table 6).

In addition, in order to verify the physical stability of the lipid nanoparticles over time, particle size and PDI evaluations were performed after 15 days of storage at 25°C. The systems developed with the T80 emulsifier, both in the presence and absence of FP, remained stable without significant difference ( $p \geq 0.05$ ) for Z-ave and PDI after 15 days (Figures 3 and 4). In the systems developed with emulsifiers S60 and SL, there were more pronounced differences ( $p \geq 0.05$ ) can be noticed in Z-ave and PDI. In general, reductions in Z-ave of the particles were observed, with consequent reduction of PDI. It should be noted that this behavior was positive for the nanoparticles developed with S60, mainly in relation to the number distribution of particles ( $N_{\text{ad}}$ ), presenting a more uniform behavior (Figure 4).

The most relevant results were obtained for the NLC+FPS60 developed with 5 cycles of HAP, showing a reduction of Z-ave from 681.70 to 288.30 nm and PDI from 0.590 to 0.307, after 15 days. Even so, by the value of PDI above 0.25, this system is still susceptible to destabilization. This behavior, related to reductions in Z-ave of the particles, has been already reported by other research groups. According to Salminen et al. [29], these Z-ave reductions commonly occur in nanostructured lipid systems developed with fully saturated TAGs, being closely related to polymorphic transitions. The authors have mentioned that the polymorphic transition tends to reach equilibrium and the transition to the more stable polymorphic form ends up occurring. In addition, the authors state that if the system is exposed to temperature changes during storage the polymorphic transition is can be easily induced.

The distributions presented in Figure 3 show that for NLCT80 and NLCS60 the size differences between cycles occurred within 24 h, with similar distributions in 15 days, as observed in I distributions. In both cases, there was a predominance of the population with diameters between 80-100 nm, according to N distribution. Therefore, as observed from the results obtained, polymorphic transitions possibly occurred during the 15 days of storage for all developed systems.

**3.2.7 Thermal behavior of NLC:** During the first NLC cooling cycle, an exothermic peak was observed at 20.09°C (NLC  $T_{pc}$ ), approximately 23°C lower than the  $T_{pc}$  of the LM used to produce the lipid nanoparticles ( $T_{pc}=43.03^\circ\text{C}$ ) (Figure 5A). Similar results were obtained by Awad et al. [1] in a study with SLN in aqueous suspension, composed of tripalmitin and polysorbate 20 as the emulsifier, using the same crystallization rate. The authors have observed that the LM has crystallized at a higher temperature ( $T_{pc}=39^\circ\text{C}$ ) than the corresponding SLN ( $T_{pc}=19^\circ\text{C}$ ). Walstra [30] explains that the conventional crystallization of macroscale materials generally occurs through the heterogeneous nucleation process, from the presence of catalytic impurities, such as monoacylglycerols in lipids. It is considered that the presence of these impurities favors the initial of crystallization. However, in emulsified

systems, such as SLN and NLC, crystallization becomes more difficult since the lipid material is finely divided into tiny droplets. Thus, the crystallization occurs into each droplet and the probability of being modulated by impurities is reduced. Thus, crystallization is not propagated as in a continuous lipid matrix, being necessary to use lower temperatures to initiate lipid crystallization in NLC.

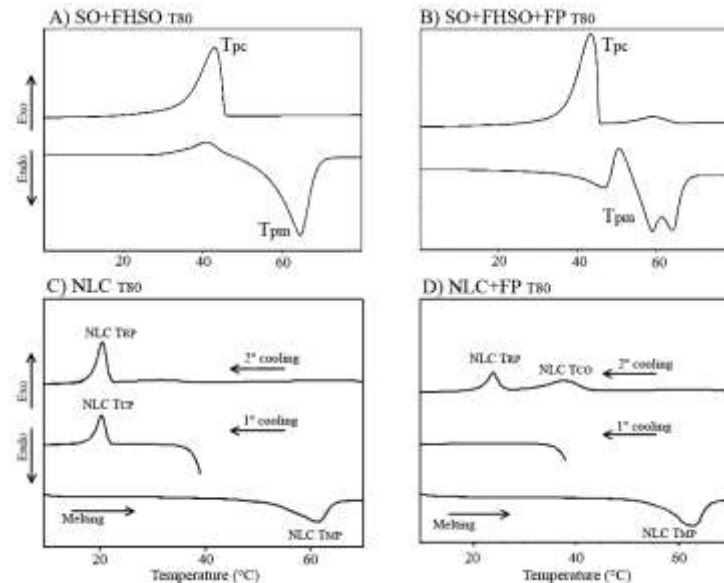


**Figure 5:** DSC thermograms of: (A) Lipid matrix composed soybean oil, SO, fully hydrogenated soybean oil, FHSO and polyethoxylated sorbitan monooleate, T80 and (B) Lipid matrix composed by SO, FHSO and T80 with incorporation of free phytosterols (FP), using temperature cycles of 75-5-75°C; (C) NLC<sub>T80</sub>-nanostructured lipid carriers composed by SO, FHSO and T80 and (D) NLC+FP<sub>T80</sub> nanostructured lipid carriers composed by SO, FHSO and T80 with incorporation of FP, using temperature cycles of 37-5-75-5°C. Where:  $T_{pc}$ =Maximum crystallization temperature of the lipid matrices;  $T_{pm}$ =Maximum melting temperature of the lipid matrices; NLC  $T_{pc}$ =Maximum crystallization temperature; NLC  $T_{pm}$ =Maximum melting temperature; CLN  $T_{pr}$ =Maximum recrystallization temperature; NLC  $T_{co}$ =Maximum lipid coalescence temperature.

In the NLC+FP no crystallization peak was observed during the first cooling cycle (Figure 5D). It has been noted that the crystallization behavior of this system is different, probably because of the presence of FP. As can be seen in Figure 5A, in the LM containing FP two crystallization peaks were observed, one of lower intensity at 59.06°C and the other at 43.48°C. This early crystallization of the components that crystallized at the higher temperature, is represented by the FP and possibly trisaturated TAG of the LM. These components have may act as crystallization inducers inside the droplets, favoring the crystallization and concluding the NLC phase transition (liquid-solid) at temperatures above 37°C. During the NLC heating cycle, only one endothermic peak was observed at 61.39°C, as well as, the corresponding LM. In the NLC+FP, also only one melting peak was observed, at approximately 63°C. However, two endothermic peaks were observed in the LM, one at approximately 48°C, followed by another crystallization peak at 60-70°C. It was observed that this last peak had two maximum points, at 60 and 65°C approximately, they probably are associated with the polymorphic transition in the LM from  $\beta'$ -form to the more

stable form ( $\beta$ ). Generally, endothermic peaks can be used to suggest about the polymorphic forms of TAGs, but these can only be confirmed by the XRD analysis discussed in the next topic.

In the second cooling cycle, performed after the melting, the peaks observed in the NLC+FP maintained a similar behavior to the LM. In addition, it was also found that the phase transition occurred at lower temperatures during this recrystallization compared to the crystallization of the LM. For NLC a different behavior was noticed during the second cooling cycle. Two recrystallization peaks were observed, one of lower intensity at  $\sim 38^\circ\text{C}$ , which may be related to the destabilization of some nanoparticles after the melting process. This phenomenon was also observed in the research developed by Awad et al. [1]. The authors reported that when the SLN composed of tripalmitin was cooled for the second time, two exothermic peaks were observed at approximately 19 and  $39^\circ\text{C}$ . The peak at  $19^\circ\text{C}$  was attributed to crystallization of NLC, while the peak at  $39^\circ\text{C}$  was attributed to a system destabilization. Thus, the first peak ( $39^\circ\text{C}$ ) was attributed to the crystallization of tripalmitin, which may be contained in large (coalesced) droplets.

Even though, it should be noted that the higher intensity recrystallization peak (NLC  $T_{pr}$ ) observed in the NLC was very close to the peak observed in the first cycle (NLC  $T_{pc} = 20.23^\circ\text{C}$  and NLC  $T_{pc} = 20.09^\circ\text{C}$ , respectively), indicating high stability of the NLC system. This NLC stability was confirmed in the evaluation of Z-ave and PDI after 15 days from processing, as already discussed.

**3.2.8 X-Ray diffraction:** The soybean oil is liquid at the analysis temperature, making it impossible to characterize by XRD. In addition, the XRD analyzes were performed for the nanoparticles obtained with 5 cycles of HPH, since they were the ones that presented the best results of Z-ave and PDI, as previously discussed.

In the results of the characterization of the raw materials through XRD, it was possible to observe FHSO a high-intensity peak for FHSO, with SS at  $4.15\text{\AA}$ , which is characteristic of the  $\alpha$ -form (Figure 6A). For the FP, evaluating from the point of view of theta-2theta system ( $\theta$ - $2\theta$ ) a series of peaks was identified: 5.20, 12.18, 12.80, 15.08, 15.80, 16.92, 17.86, 18.64, 19.70, 20.88, 21.82, 22.96, 24.06 and  $25.28\text{\AA}$ . Among these, the peaks of higher intensities were highlighted in Figure 5E and were similar to those found by Hariklia Vaikousi et al. [9]. It should be noted that some diffraction peaks are very similar to those used for the identification of the TAG polymorphs. The atoms of the TAG molecules have regular distances between them, already established and well documented in the scientific literature, allowing the identification of polymorphic forms  $\alpha$  in 0.41 nm,  $\beta'$  in 0.42 and 0.38 nm and  $\beta$  with high peak intensity at 0.46 nm and lower intensity at 0.38 and 0.37 nm [11]. For this reason, depending on the percentage of FP incorporated in LM and NLC, the FP can interfere in the identification of TAG polymorphic forms.

Evaluating the diffraction patterns of the LM (Figure 5B and 5F), it was possible to observe diffraction peaks at SS 4.2 and  $3.8\text{\AA}$  characteristics of the  $\beta'$ -form and also in  $4.6\text{\AA}$ , SS that characterizes the presence of crystals in the  $\beta$ -

form. In this way, it was observed that in these lipid matrices, there is a mixture of crystals in both  $\beta'$  and  $\beta$  forms, indicating that these materials are in polymorphic transition. Ribeiro et al. [31] also characterize mixtures of SO with FHSO, in the same proportion used in our studies (50:50 mm) and observe the simultaneous presence of  $\beta'$  and  $\beta$  crystals. Except for the LM developed with FP and S60 (Figure 6F), where only the characteristic SS of the most stable polymorphic form,  $\beta$ , were observed. Probably, the polymorphic transitions were facilitated by the presence of the S60 emulsifier.

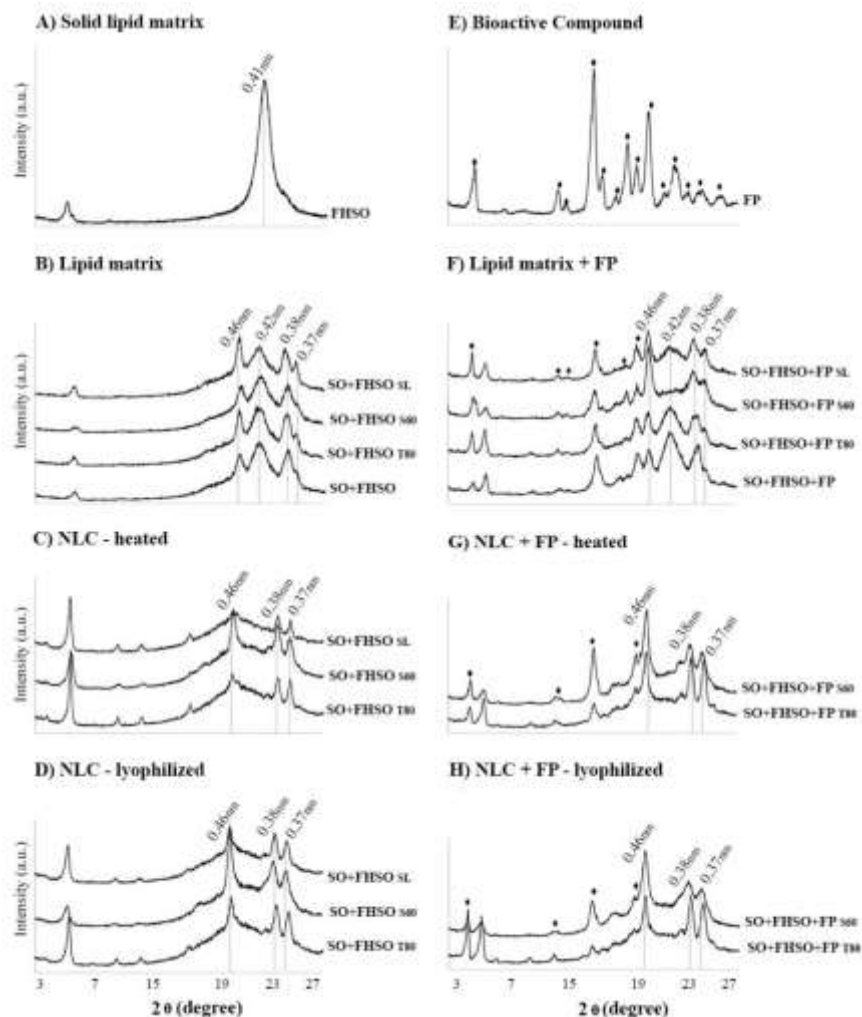


**Figure 6:** X-ray diffraction patterns obtained at 25°C: A) Fully hydrogenated soybean oil-FHSO; B) Lipid matrices developed with different emulsifiers (soybean lecithin-SL, polyethoxylated sorbitan monooleate-T80 and sorbitan monostearate-S60) used in the NLC production; C) nanostructured lipid carriers-NLC heated (oven dried); D) NLC lyophilized; E) Free phytosterols-FP; F) Lipid matrix with free phytosterols and different emulsifiers (SL, T80 and S60) used in the NLC+FP; G) NLC+FP heated (oven dried), and H) NLC+FP lyophilized.

In the diffractograms corresponding to the NLC and NLC+FP obtained after the oven drying (Figure 6C and 6G) and lyophilization (Figure 5D and 5H), it was possible to observe only SS characteristics of crystals in the  $\beta$ -form. Thus, it can be affirmed that the polymorphic transitions were facilitated in the nanoparticles as compared to the

corresponding LM. It is noteworthy that both were subjected to the same crystallization conditions and XRD analysis. Thus, it is suggested that the stabilization in the  $\beta$ -form may be related to the additional processes of nanoparticles drying. Salminen et al. [30] described that polymorphic transitions in the nanoparticles are facilitated when temperature increases in the system. However, the results obtained here showed that after both drying treatments, crystals were observed in the most stable form ( $\beta$ ). Moreover, for NLC+FP, similar diffractograms were obtained for lyophilized and oven dried nanoparticles (Figure 5G and 5H). Being the SS at 4.6 nm, characterized as very strong intensity for the NLC+FP with S60 and of medium intensity, for the NLC+FP containing T80 (Table 7). The drying process did not interfere in the NLC+FP polymorphism. However, the different emulsifiers were found to interfere in the NLC+FP crystallinity, the systems developed with the T80 emulsifier were less crystalline when compared to those containing S60 (Figure 5H and 5G).

Lipid matrices	Short spacing (nm)					TAG Polymorphic form
	0.46	0.41	0.42	0.38	0.36	
FHSO	-	0.406 <sub>s</sub>	-	-	-	$\alpha$
SO+ FHSO	0.443 <sub>M</sub>	-	0.412 <sub>M</sub>	0.370 <sub>M</sub>	-	$\beta' + \beta$
SO+ FHSO+FP	0.449 <sub>M</sub>	-	0.414 <sub>s</sub>	0.371 <sub>M</sub>	0.362 <sub>vw</sub>	$\beta' + \beta$
SO+ FHSO <sub>T80</sub>	0.445 <sub>M</sub>	-	0.412 <sub>M</sub>	0.373 <sub>M</sub>	0.361 <sub>vw</sub>	$\beta' + \beta$
SO+ FHSO <sub>S60</sub>	0.442 <sub>M</sub>	-	0.411 <sub>M</sub>	0.372 <sub>M</sub>	-	$\beta' + \beta$
SO+ FHSO <sub>SL</sub>	0.447 <sub>F</sub>	-	0.412 <sub>M</sub>	0.375 <sub>M</sub>	0.362 <sub>w</sub>	$\beta' + \beta$
SO+ FHSO+FP <sub>T80</sub>	0.450 <sub>M</sub>	-	0.414 <sub>s</sub>	0.377 <sub>M</sub>	0.365 <sub>vw</sub>	$\beta' + \beta$
SO+ FHSO+FP <sub>S60</sub>	0.449 <sub>vw</sub>	-	-	0.380 <sub>M</sub>	0.366 <sub>w</sub>	$\beta$
SO+ FHSO+FP <sub>SL</sub>	0.451 <sub>s</sub>	-	0.413 <sub>vw</sub>	0.379 <sub>M</sub>	-	$\beta' + \beta$
<b>NLC heated</b>						
NLC <sub>T80</sub>	0.456 <sub>vw</sub>	-	-	0.382 <sub>M</sub>	0.366 <sub>M</sub>	$\beta$
NLC <sub>S60</sub>	0.452 <sub>s</sub>	-	-	0.382 <sub>M</sub>	0.365 <sub>M</sub>	$\beta$
NLC <sub>SL</sub>	0.456 <sub>vw</sub>	-	-	0.382 <sub>M</sub>	0.366 <sub>M</sub>	$\beta$
NLC+FP <sub>T80</sub>	0.454 <sub>vs</sub>	-	-	0.382 <sub>vs</sub>	0.365 <sub>vs</sub>	$\beta$
NLC+FP <sub>S60</sub>	0.453 <sub>vs</sub>	-	-	0.383 <sub>M</sub>	0.367 <sub>M</sub>	$\beta$
<b>NLC lyophilized</b>						
NLC <sub>T80</sub>	0.457 <sub>M</sub>	-	-	0.384 <sub>M</sub>	0.368 <sub>M</sub>	$\beta$
NLC <sub>S60</sub>	0.460 <sub>vs</sub>	-	-	0.388 <sub>M</sub>	0.371 <sub>M</sub>	$\beta$
NLC <sub>SL</sub>	0.460 <sub>M</sub>	-	-	0.387 <sub>M</sub>	0.370 <sub>M</sub>	$\beta$
NLC+FP <sub>T80</sub>	0.459 <sub>M</sub>	-	-	0.386 <sub>M</sub>	0.369 <sub>M</sub>	$\beta$
NLC+FP <sub>S60</sub>	0.460 <sub>vs</sub>	-	-	0.389 <sub>w</sub>	0.371 <sub>w</sub>	$\beta$

Peak intensity: V-very; W-weak; M-medium; S-strong

**Table 7:** Triacylglycerols polymorphic forms, short spacings and peak intensities in the diffractogram from lipid matrices and NLC obtained through 3 cycles of HPH, heated (oven dried) and lyophilized.

On the other hand, polymorphic transitions of  $\beta'$  to  $\beta$  were hampered in the oven drying process of the NLC (Figure 6C and 5D). It was mainly observed in the systems developed with SL and T80, which presented very weak intensities of SS peaks at 4.6Å, referring to the  $\beta$ -form (Table 7). Probably, partial melting of some TAGs, of an intermediate melting point, may have occurred during the heating, drying, hindering the mobility of the crystalline structure to the most stable form ( $\beta$ ). This was not observed in the nanoparticles developed with FP, because they presented higher thermal resistance due to the high melting point of FP. Finally, the obtaining of nanostructured systems in the  $\beta$ -form, which is the most stable form, guarantees that during the application of these systems in food, no more polymorphic transitions will occur, which could be associated to the destabilization of the product during storage.

#### 4. Conclusion

SO and FHSO were found to be compatible materials for the development of NLC and NLC+FP. The HPH process was effective to obtain the NLC and NLC+FP, mainly by maintaining the high temperature of the systems during processing, avoiding the crystallization of the solid lipids and FP. The number of HPH cycles did not interfere with the particle size and polydispersity of the nanoparticles, but it did contribute to PDI reduction in the NLC+FP. The T80 was more effective in the stabilization of the systems, providing the smallest values of size and polydispersity for the nanoparticles. The nanoparticles in aqueous dispersion, compared to the LM, required lower temperatures for crystallization. The systems developed with FP presented higher thermal resistance. The polymorphic transitions were accelerated after the drying processes, with crystals predominating in the  $\beta$ -form. The drying method did not interfere in the polymorphism of carriers with FP, but for those without FP, the polymorphic transitions were hampered in the oven drying process. In addition, in both NLC and NLC+FP, the systems with T80 were less crystalline. Thus, it can be concluded that the systems developed are innovative systems, mainly in terms of compositions of LM and present a high potential for food applications. We suggest the use of NLC+FP in aqueous based foods, where FP dispersion is hampered by their high melting point and limited solubility. In addition, it's possible to apply the oven dried or lyophilized NLC, as crystallization seeds in lipid-based foods, for the induction of  $\beta$ -form.

#### Acknowledgements

The authors are thankful for the financial support of the Foundation for Research Support of the State of São Paulo (FAPESP, Brazil) referring to the process 16/11261-8 and the doctoral scholarship from the Coordination for the Improvement of Higher Personnel Education (CAPES, Brazil).

#### Conflicts of Interest

The authors declare that they have no known competing financial interests or personal relationships that could have appeared to influence the work reported in this paper.

## References

1. Awad TS, Helgason T, Weiss J, et al. Effect of Omega-3 Fatty Acids on Crystallization, Polymorphic Transformation and Stability of Tripalmitin Solid Lipid Nanoparticle Suspensions. *Crystal Growth and Design* 9 (2009): 3405-3411.
2. McClements DJ. Edible lipid nanoparticles: Digestion, absorption, and potential toxicity. *Progress in Lipid Research* 52 (2013): 409-423.
3. Santos VS, Ribeiro APB, Santana MH. Solid lipid nanoparticles as carriers for lipophilic compounds for applications in foods. *Food Research International* (2019): DOI: 10.1016/j.foodres.2019.01.032.
4. Severino P, Andreani T, Macedo AS, et al. Current State-of-Art and New Trends on Lipid Nanoparticles (SLN and NLC) for Oral Drug Delivery. *Journal of Drug Delivery* 2012 (2012): 750891.
5. Ganesan P, Narayanasamy D. Lipid nanoparticles: Different preparation techniques, characterization, hurdles, and strategies for the production of solid lipid nanoparticles and nanostructured lipid carriers for oral drug delivery 6 (2017): 37-56.
6. Mehnert W, Mader K. Solid lipid nanoparticles. *Advanced Drug Delivery Reviews* 64 (2012): 83-101.
7. Ribeiro APB, Basso RC, Kieckbusch TG. Effect of the addition of hardfats on the physical properties of cocoa butter. *European Journal of Lipid Science and Technology* 115 (2013): 301-312.
8. Chaves KF, Barrera-Arellano D, Ribeiro APB. Potential application of lipid organogels for food industry. *Food Res Int* 105 (2018): 863-872.
9. Hariklia Vaikousi, Athina Lazaridou, Costas G Biliaderis, et al. Phase Transitions, Solubility, and Crystallization Kinetics of Phytosterols and Phytosterol-Oil Blends. *J. Agric. Food Chem* 55 (2007): 1790-1798.
10. Shahzad N, Khan W, Md S, et al. Phytosterols as a natural anticancer agent: Current status and future perspective. *Biomed Pharmacother* 88 (2017): 786-794.
11. Gomes Silva M, Santos VS, Fernandes GD, et al. Physical approach for a quantitative analysis of the phytosterols in free phytosterol-oil blends by X-ray Rietveld method. *Food Research International* (2019): <https://doi.org/10.1016/j.foodres.2019.04.006>.
12. Sato K. Crystallization behaviour of fats and lipids: a review. *Oxford* 56 (2001): 2255-2265.
13. Santos VS, Ribeiro APB, Santana MHA. Nanoparticulas Lipídicas Sólidas (NLS) e Carreadores Lipídicos Nanoestruturados (CLN) para aplicacao em alimentos, processo para obtencao de NLS e CLN e uso das NLS e dos CLN. In: Unicamp, Editor INPI-Instituto Nacional da Propriedade Industrial. Brasil (2017): 40.
14. AOCS. Official methods and recommended practices of the American Oil Chemists' Society. Urbana (USA): AOCS Press (2009).
15. Hartman L, Lago R. Rapid preparation of fatty acid methyl esters from lipids. *Laboratory Practice* 22 (1973): 475-476.
16. Antoniosi FNR, Mendes OL, Lancas FM. Computer prediction of triacylglycerol composition of vegetable

- oils by HRGC. *Chromatographia* 40 (1995): 557-562.
17. Zimmermann E, Muller RH, Mader K. Influence of different parameters on reconstitution of lyophilized SLN. *International Journal of Pharmaceutics* 196 (2000): 211-213.
  18. Campos R. Experimental methodology. In: Marangoni A, Editor *Fat Crystal Networks*. New York: Marcel Dekker (2005): 267-349.
  19. Ribeiro APB, Grimaldi R, Gioielli LA, et al. Zero trans fats from soybean oil and fully hydrogenated soybean oil: Physico-chemical properties and food applications. *Food Research International* 42 (2009): 401-410.
  20. Regitano-D'arce MAB, Vieira TMFS. Fuentes de Aceites y Grasas. In: Block JM, Barrera-Arellano D, Editors. *Temas Selectos en Aceites y Grasas-Volumen 1/ Procesamiento*. Sao Paulo: Blucher (2009): 1-29.
  21. O'Brien RD. *Fats and oils formulation*. Boca Raton: CRC Press (2009).
  22. Ribeiro APB, Masuchi MH, Grimaldi R, et al. Interesterificação química de óleo de soja e óleo de soja totalmente hidrogenado: influência do tempo de reação. *Química Nova* 32 (2009): 939-945.
  23. Gomez-Coca RB, Perez-Camino MC, Moreda W. Analysis of Neutral Lipids: Unsaponifiable Matter. In: Nollet L, Toldrá F, Editors. *Handbook of Food Analysis*. Boca Raton, Florida, USA: CRC Press (2015).
  24. Mensink RP. Effects of stearic acid on plasma lipid and lipoproteins in humans. *Lipids* 40 (2005): 1201-1205.
  25. Tamjidi F, Shahedi M, Varshosaz J, et al. Nanostructured lipid carriers (NLC): A potential delivery system for bioactive food molecules. *Innovative Food Science and Emerging Technologies* 19 (2013): 29-43.
  26. Muller RH, Runge S, Ravelli V, et al. Oral bioavailability of cyclosporine: solid lipid nanoparticles (SLN) versus drug nanocrystals. *International Journal of Pharmaceutics* 317 (2011): 82-89.
  27. Oliveira GM, Stahl MA, Ribeiro APB, et al. Development of zero trans/low sat fat systems structured with sorbitan monostearate and fully hydrogenated canola oil. *European Journal of Lipid Science and Technology* 117 (2015): 1762-1771.
  28. Engel R, Schubert H. Formulation of phytosterols in emulsions for increased dose response in functional foods. *Innovative Food Science and Emerging Technologies* 6 (2005): 233-237.
  29. Salminen H, Helgason T, Kristinsson B, et al. Formation of solid shell nanoparticles with liquid omega-3 fatty acid core. *Food Chemistry* 141 (2013): 2934-2943.
  30. Walstra P. *Physical chemistry of foods*. New York [etc.]: Marcel Dekker (2003).
  31. Ribeiro APB, Grimaldi R, Gioielli LA, et al. Thermal Behavior, Microstructure, Polymorphism, and Crystallization Properties of Zero Trans Fats from Soybean Oil and Fully Hydrogenated Soybean Oil. *Food Biophysics* 4 (2009): 106-118.

**Citation:** Valeria da Silva Santos, Eriksen Koji Miyasaki, Lisandro Pavie Cardoso, Ana Paula Badan Ribeiro, Maria Helena Andrade Santana. Crystallization, Polymorphism and Stability of Nanostructured Lipid Carriers Developed with Soybean Oil, Fully Hydrogenated Soybean Oil and Free Phytosterols for Food Applications. *Journal of Nanotechnology Research* 2 (2019): 001-022.



This article is an open access article distributed under the terms and conditions of the [Creative Commons Attribution \(CC-BY\) license 4.0](https://creativecommons.org/licenses/by/4.0/)